Battery Management Systems

Accurate State-of-Charge Indication for Battery-Powered Applications

Philips Research

VOLUME 9

Editor-in-Chief
Dr. Frank Toolenaar
Philips Research Laboratories, Eindhoven, The Netherlands

SCOPE TO THE *'PHILIPS RESEARCH BOOK SERIES'*

As one of the largest private sector research establishments in the world, Philips Research is shaping the future with technology inventions that meet peoples' needs and desires in the digital age. While the ultimate user benefits of these inventions end up on the high-streeet shelves, the often pioneering scientific and technological basis usually remains less visisble.

This 'Philips Research Book Series' has been set up as a way for Philips researchers to contribute to the scientific community by publishing their comprehensive results and theories in book form.

Dr. Rick Harwig

Battery Management Systems

Accurate State-of-Charge Indication for Battery-Powered Applications

by

Valer Pop
Holst Centre/IMEC-NL
Eindhoven, The Netherlands

Henk Jan Bergveld
NXP Semiconductors
Eindhoven, The Netherlands

Dmitry Danilov
Eurandom, Eindhoven
The Netherlands

Paul P.L. Regtien
University of Twente
Enschede, The Netherlands

and

Peter H.L. Notten
Philips Research Laboratories Eindhoven
Eindhoven University of Technology
Eindhoven, The Netherlands

Springer

Valer Pop
Holst Centre/IMEC-NL
Eindhoven, The Netherlands

Henk Jan Bergveld
NXP Semiconductors
Eindhoven, The Netherlands

Dmitry Danilov
Eurandom
Eindhoven, The Netherlands

Paul P.L. Regtien
University of Twente
Enschede, The Netherlands

Peter H.L. Notten
Philips Research Laboratories Eindhoven
Eindhoven University of Technology
Eindhoven, The Netherlands

ISBN 978-1-4020-6944-4 e-ISBN 978-1-4020-6945-1

Library of Congress Control Number: 2008921935

Printed on acid-free paper.

9 8 7 6 5 4 3 2 1

springer.com

To Raluca, Peggy, Olga, Elly and Pascalle

Table of contents

List of abbreviations

ADC	Analog-to-Digital Converter
ANN	Artificial Neural Networks
AR_d	Actual Rate discharge current
ACU	Adaptive Control Unit
b	Boostcharge
BMS	Battery Management System
BKM	Book-Keeping Module
cc	Coulomb counting
CC	Constant-Current
CCCV	Constant-Current-Constant-Voltage
CCCVCCCV	$(CCCV)^2$
CD	Compact Disc
C_n	Cycle number
ch	Charge
CCA	Charging Current Accumulator
CAC	Compensated Available Charge
d	Discharge
DAC	Digital-to-Analog Converter
DCA	Discharging Current Accumulator
DAQ	Data Acquisition interface card
Dig. I/O	Digital Input/Output pins
EIS	Electrochemical Impedance Spectroscopy
EMF_{dt}	EMF detection method
EMF_f	EMF fitting method
EKF	Extended Kalman Filters
EEPROM	Electrically Erasable Read-Only Memory
EMF_m	Measured EMF data points
f_{sd}	Self-discharge rate estimation rate
GUI	Graphical User Interface
GITT	Galvanostatic Intermittent Titration Technique
HDQ	High-speed single-wire interface
HEV	Hybrid Electrical Vehicles
ISP	In-System Programming
IF	In-Functional
IC	Integrated Circuit
I^2C	Inter-Integrated-Circuit Bus
ICA	Integrated Current Accumulator
JTAG	Joint Test Action Group
KF	Kalman Filters
LED	Light-Emitting Diode
LCD	Liquid-Crystal Display
Li-ion	Lithium-ion
LA	Lead-Acid
Li-ion POL	Lithium-ion Polymer
$Li\text{-}SO_2$	Lithium–Sulphur Dioxide
Li	Lithium
LCR	Learning Count Register

LMD	Last Measured Discharge
NiCd	Nickel–Cadmium
NiMH	Nickel–Metal Hydride
NI	National Instruments
NAC	Nominal Available Charge
NTC	Negative-Temperature-Coefficient
N	Number of ADC bits
OLS	Ordinary Least Squares
PGA	Programmable Gain Amplifier
PM	Power Module
ph	Phase transition
PC	Personal Computer
RTOS	Real-Time Operating System
ROM	Read-Only Memory
RAM	Random-Access Memory
SoH	State-of-Health
SBS	Smart Battery System
sd	Self-discharge
SEI	Solid Electrolyte Interface
SCB-68	National Instruments connector board
SPI	Serial Peripheral Interface
UART	Universal Asynchronous Receiver Transmitter
V_{pm}	Voltage prediction model
VDQ	Valid Discharge flag
η_m	Overpotential model

List of symbols

Symbol	Meaning	Value	Unit
a	aged		–
A	Parameter for the SoC-EMF relationship modelling		[1]
a_{10}	Parameter for the SoC-EMF relationship modelling		[1]
a_{11}	Parameter for the SoC-EMF relationship modelling		[1]
a_{12}	Parameter for the SoC-EMF relationship modelling		[1]
a_{20}	Parameter for the SoC-EMF relationship modelling		[1]
a_{21}	Parameter for the SoC-EMF relationship modelling		[1]
a_{22}	Parameter for the SoC-EMF relationship modelling		[1]
c_o	Parameter for overpotential modelling		$[\Omega\ A^{-1}]$
c_1	Parameter for overpotential modelling		[V]
c_2	Parameter for overpotential modelling	1	$[\sqrt{s}]$
c_3	Parameter for overpotential modelling		[J]
c_4	Parameter for overpotential modelling	1	$[A^{-1}]$
c_5	Parameter for overpotential modelling		[A]
C_d	Mean discharge C-rate current		–
DoD	Depth-of-Discharge		[%]
DoC	Depth-of-Charge		[%]
EMF	Electro-Motive Force		[V]
E_q^o	Amount of the energy that cannot be obtained from the battery		[J]
E_q^I	Non-linear part of the amount of the energy that cannot be obtained from the battery		[J]
E_{eq}^+	Equilibrium potential of the positive electrode		[V]
E_{eq}^-	Equilibrium potential of the negative electrode		[V]

Symbol	Meaning	Value	Unit
E_0^+	Standard redox potential of the positive electrode		[V]
E_0^-	Standard redox potential of the negative electrode		[V]
EDV_1	End-of Discharge Voltage level		[V]
EMF_m^{es}	Estimated EMF model		[V]
$EMF_{a5.4\%}$	EMF obtained for the 5.4% capacity loss battery (a=aged)		
$EMF_{a25.4\%}$	EMF obtained for the 25.4% capacity loss battery (a=aged)		
EMF_1	First EMF point determined for the EMF adaptation		[V]
EMF_{ad}	EMF retrieved by means of the adaptation method		[V]
E_0	Parameter for the SoC-EMF relationship modelling		[V]
EMF_p	Predicted EMF voltage		[V]
EMF_{GITT}	EMF measurement by means of the GITT		
EMF_f	Fitted EMF		[V]
F	Faraday constant	96485	[C mol^{-1}]
f	Frequency		[Hz]
f	Fresh		–
I_s^{max}	Constant maximum current (s=standard)		[A]
I_s^{min}	Predefined minimum current (s=standard)		[A]
I_b^{max}	Maximum boostcharging current		[A]
I	Current that flows into(out) of the battery		[A]
I_M	Uncertainties from Maccor current measurements	Neglected	[A]
I_s	Standby current	$-1\ 10^{-3}$	[A]
I_b	Backlight-on state current		[A]
I_d	Measured discharge current		[A]
I_{lim}	Limit current		[A]
M	Slope of second asymptote of prior-art voltage-prediction method		–
n_0	Parameter related to the magnitude of the diffusion overpotential		[1]
n_1	Parameter related to the magnitude of the diffusion overpotential		[T^{-1}]

Symbol	Meaning	Value	Unit
OCV	Open-Circuit Voltage		[V]
OCV_f	Battery OCV for a fresh battery		[V]
OCV_a	Battery OCV for an aged battery		[V]
$par(T_{ref})$	Value of one of the EMF-SoC model parameters at temperature T_{ref}		[1]
p_{11}	Parameter for the SoC-EMF relationship modelling		[1]
p_{12}	Parameter for the SoC-EMF relationship modelling		[1]
p_{21}	Parameter for the SoC-EMF relationship modelling		[1]
p_{22}	Parameter for the SoC-EMF relationship modelling		[1]
q_{11}	Parameter for the SoC-EMF relationship modelling		[1]
q_{12}	Parameter for the SoC-EMF relationship modelling		[1]
q_{21}	Parameter for the SoC-EMF relationship modelling		[1]
q_{22}	Parameter for the SoC-EMF relationship modelling		[1]
Q_{in}	Charge present in the battery at the time t		[Ah]
Q_{d2}	Discharge capacity for battery number 2		[Ah]
Q_{d1}	Discharge capacity for battery number 1		[Ah]
Q_{d1}^{1}	Q_{d1} value after the first cycle	$1165\ 10^{-3}$	[Ah]
Q_{d1}^{220}	Q_{d1} value after 220 cycles	$675\ 10^{-3}$	[Ah]
Q_{d2}^{1}	Q_{d2} value after the first cycle	$1150\ 10^{-3}$	[Ah]
Q_{d2}^{2000}	Q_{d2} value after 2000 cycles	$935\ 10^{-3}$	[Ah]
Q_{max}	Battery maximum capacity		[Ah]
Q_{max1}	Maximum capacity of battery 1	$875\ 10^{-3}$	[Ah]
Q_{max2}	Maximum capacity of battery 2	$1110\ 10^{-3}$	[Ah]
Q_{loss}	Capacity loss		[%]
Q_d	Discharge battery capacity		[Ah]
Q_{dd}	Decrease in Q_d		[%]
Q_{max}^{+}	Maximum capacity of the positive electrode	1.00	[1]
Q_{max}^{-}	Maximum capacity of the negative electrode	$4.23\ 10^{-1}$	[1]

Symbol	Meaning	Value	Unit
Q_{max}	Amount of the electrochemically active Li^+ ions inside the battery	$8.11\ 10^{-1}$	[1]
Q_{maxr}	Reference maximum capacity value	$1173\ 10^{-3}$	[Ah]
Q_0^-	Amount of the Li^+ ions that will remain in the negative electrode after discharging	$9.63\ 10^{-4}$	[1]
Q_{ch}	Amount of charge flowing into the battery during the charge state		[Ah]
Q_d	Discharge capacity		[Ah]
R	Gas constant	8.314	$J(mol\ K)^{-1})$
R	Resistance		[Ω]
R_d^0	Linear contribution of the “diffusion” resistance		[Ω]
R_d^I	Non-linear contribution of the “diffusion” resistance		[Ω]
R_S	Sense resistor	$20\ 10^{-3}$	[Ω]
$R_{\Omega k}$	Linear contribution of the “ohmic” and “kinetic” resistance		[Ω]
R_{Ik}	Non-linear contribution of the “ohmic” and “kinetic” resistance		[Ω]
R_{HF}	High-frequency resistance		[Ω]
s_x	Sign of parameter x		–
SoC	State-of-Charge		[%]
SoC(EMF)	SoC calculated based on the EMF voltage		[%]
$SoC(V_p)$	SoC calculated based on the predicted voltage		[%]
SoC_l	SoC-left		[%]
SoC_{lm}^{es}	Estimated SoC_l model		[%]
SoC_{lm}	Measured SoC_l		[%]
SoC_{lf}	Fitted SoC_l		[%]
SoC_e	SoC error		[%]
SoC_{si}	Initial SoC in the standby state		[%]
SoC_{sf}	Final SoC in the standby state		[%]
SoC_{st}	SoC indicated at the start		[%]
SoC_{end}	SoC indicated at the end		[%]
SoC_{in}	SoC in the initial state		[%]
SoCs	SoC in the standby state		[%]
SoC_t	SoC in the transitional state		[%]
SoC_{ch}	SoC in the charge state		[%]
SoC_d	SoC in the discharge state		[%]
SoC_b	SoC in the backlight-on state		[%]

Symbol	Meaning	Value	Unit
$SoC_e(V_p)$	Error of the SoC calculated based on a predicted voltage		[%]
SoC_e (OCV)	Error of the SoC calculated based on the OCV		[%]
t	time		[s]
T	Temperature		[°C]
T_{ref}	Reference temperature	25	[°C]
t_b	Time boostcharging		[min]
t_{empty}	Time where battery is empty		[min]
t_r	Remaining run-time		[min]
t_{rst}	Remaining run-time at the start of experiment		[min]
t_{re}	Error in the remaining run-time at the end of the experiment		[min]
t_{rstp}	Predicted remaining run-time at the start of the experiment		[min]
t_{rstm}	Measured remaining run-time at the start of the experiment		[min]
t_{rre}	Relative error in the remaining run-time		[%]
T_M	Uncertainties from Maccor temperature measurements	Neglected	[°C]
t_M	Uncertainties from Maccor time measurements	Neglected	[s]
U_1^+	Interaction energy coefficient of the positive electrode	$9.68\ 10^2$	[1]
U_2^+	Interaction energy coefficient of the positive electrode	$1.63\ 10^4$	[1]
U_1^-	Interaction energy coefficient of the negative electrode	$-6.92\ 10^3$	[1]
U_2^-	Interaction energy coefficient of the positive electrode	$-6.89\ 10^3$	[1]
U_j^-	Interaction energy coefficient of the negative electrode		–
U_j^+	Interaction energy coefficient of the positive electrode		–
V_{bat}	Battery terminal voltage		[V]
V	Battery voltage		[V]
V_d	Battery voltage after discharging		[V]
V_{ch}	Battery voltage after charging		[V]
V_M	Uncertainties from Maccor voltage measurements	Neglected	[V]
V_o	Battery voltage at t=1min		[V]

Symbol	Meaning	Value	Unit
V_p	Predicted voltage		[V]
V_{EoD}	End-of-Discharge voltage	3	[V]
V_{ocf}	Fully stabilized Open-Circuit Voltage		[V]
V_b^{max}	Maximum boostcharging voltage		[V]
V_s^{max}	Maximum charge voltage in CV mode	4.2	[V]
V_∞	Final relaxation voltage		[V]
V_t	Relaxation voltage at time t		[V]
V_m	Measured voltage in the first 5 minutes of the relaxation		[V]
V_{off}	Voltage offset		[V]
V_{abs}	Absolute voltage accuracy at full scale	$0.95\ 10^{-3}$	[V]
V_{fs}	Full-scale range of the ADC voltage		[V]
x	Parameter for the SoC-EMF relationship modelling		–
X	Exponent of time		–
x_{Li}	Molfraction of Li^+ ions inside the positive electrode		[1]
X_p	Value of X at asymptotes intersection	1.64	–
w_2	Parameter for the SoC-EMF relationship modelling		[1]
Z	Battery impedance		[Ω]
z_{Li}	Molfraction of the Li ions inside the negative electrode		–
z_{ph}	Phase transition in the negative electrode	$4.44\ 10^{-1}$	[1]
x_{ph}	Phase transition in the positive electrode	$8.44\ 10^{-1}$	[1]
ΔU_1^+	Sensitivity to temperature of parameter U_1^+	–1.89	$[T^{-1}]$
ΔU_2^+	Sensitivity to temperature of parameter U_2^+	$5.14\ 10^1$	$[T^{-1}]$
ΔU_1^-	Sensitivity to temperature of parameter U_1^-	$2.18\ 10^1$	$[T^{-1}]$
ΔU_2^-	Sensitivity to temperature of parameter U_2^-	$2.16\ 10^1$	$[T^{-1}]$

Symbol	Meaning	Value	Unit
$\Delta\zeta_1^+$	Sensitivity to temperature of parameter ζ_1^+	$2.22\ 10^{-4}$	$[T^{-1}]$
$\Delta\zeta_1^-$	Sensitivity to temperature of ζ_1^-	$2.04\ 10^{-4}$	$[T^{-1}]$
Δx_{ph}	Sensitivity to temperature of x_{ph}	$1.58\ 10^{-6}$	$[T^{-1}]$
Δz_{ph}	Sensitivity to temperature of z_{ph}	$1.37\ 10^{-4}$	$[T^{-1}]$
$\Delta\sigma_{x1}$	Sensitivity to temperature of σ_{x1}	$-2.24\ 10^{-6}$	$[T^{-1}]$
$\Delta\sigma_{z1}$	Sensitivity to temperature of σ_{z1}	$8.98\ 10^{-4}$	$[T^{-1}]$
ΔQ_0^-	Sensitivity to temperature of Q_0^-	$4.34\ 10^{-5}$	$[T^{-1}]$
ΔA	Sensitivity to temperature of A		$[T^{-1}]$
Δw_2	Sensitivity to temperature of w_2		$[T^{-1}]$
ΔV_{max}	Maximum error in the voltage measurement		[V]
Δa_{20}	Sensitivity to temperature of a_{20}		$[T^{-1}]$
Δa_{10}	Sensitivity to temperature of a_{10}		$[T^{-1}]$
Δa_{11}	Sensitivity to temperature of a_{11}		$[T^{-1}]$
Δa_{12}	Sensitivity to temperature of a_{12}		$[T^{-1}]$
Δp_{11}	Sensitivity to temperature of p_{11}		$[T^{-1}]$
Δp_{12}	Sensitivity to temperature of p_{12}		$[T^{-1}]$
Δp_{21}	Sensitivity to temperature of p_{21}		$[T^{-1}]$
ΔE_0	Sensitivity to temperature of E_0		$[V\ T^{-1}]$
Δpar	Sensitivity to temperature determined for each parameter $par(T_{ref})$		$[T^{-1}]$
α	Rate-determining variable		–
γ	Rate-determining variable		–
δ	Rate-determining variable		–
δ	Parameter in the voltage prediction model		–
ε_t	Random error term		–
Γ	Constant for voltage prediction	+1 (discharge) –1 (charge)	–
ζ_j^+	Constant in the positive electrode		–
ζ_j^-	Constant in the negative electrode		–
ζ_1^+	Constant in the positive electrode	0.00	[1]

Symbol	Meaning	Value	Unit
ζ_1^-	Constant in the negative electrode	$-2.14\ 10^{-5}$	[1]
η_{ch}	Charge overpotential		[V]
η_d	Discharge overpotential		[V]
η_{meas}	Measured overpotential from V and EMF		[V]
η_{calc}	Calculated overpotential		[V]
η_f	Overpotential model parameters for a fresh battery		
η_{df}	Measured discharge overpotential for fresh battery		[V]
η_{chf}	Measured charge overpotential for fresh battery		[V]
η_{ch}^a	Measured charge overpotential for an aged battery		[V]
η_{ch}^f	Measured charge overpotential for a fresh battery		[V]
η_d^a	Measured discharge overpotential for an aged battery		[V]
η_d^f	Measured discharge overpotential for a fresh battery		[V]
ϕ	Phase angle		[rad]
Φ	Standard normal cumulative distribution function		–
τ_q	Time constant associated with the increase in overpotential in an almost empty battery		[s]
τ_d	“Diffusion” time constant		[s]
σ_{x1}	Parameter that determine the smoothness of the phase transition for the positive electrode	$1.72\ 10^{-2}$	[1]
σ_{z1}	Parameter that determine the smoothness of the phase transition for the negative electrode EMF	$1.22\ 10^{-1}$	[1]
τ	Voltage relaxation time		[s]

Chapter 1
Introduction

This chapter gives general information on Battery Management Systems (BMSs) and State-of-Charge (SoC) indication that will be required as a background in later chapters. A general block diagram of a BMS is shown in section 1.1. One of the main tasks of a BMS is to keep track of a battery's SoC, which is the main subject of this book. Section 1.2 gives a definition of SoC indication and discusses its importance. The goal and motivation of the research described in this book are discussed in section 1.3. Finally, section 1.4 presents the contents of this book.

1.1 Battery Management Systems

Battery-powered electronic devices have become ubiquitous in modern society. The recent rapid expansion of the use of portable devices (*e.g.* portable computers, personal data assistants, cellular phones, shavers, *etc.* (see Fig. 1.1)) and Hybrid Electrical Vehicles (HEVs) creates a strong demand for fast deployment of battery technologies at an unprecedented rate [1].

Fig. 1.1. Examples of portable devices on the market [2].

V. Pop et al., *Battery Management Systems. Accurate State-of-Charge Indication for Battery-Powered Applications.*
doi: 10.1007/978-1-4020-6945-1_1, © Springer Science + Business Media B.V. 2008

The design of a battery-powered device requires many battery-management features, including charge control, battery-capacity monitoring, remaining run-time information, charge-cycle counting, *etc.* For it to be able to offer high precision, each part of the system must be near to perfection. The basic task of a BMS can be defined as follows [1]:

The basic task of a Battery Management System (BMS) is to ensure that optimum use is made of the energy inside the battery powering the portable product and that the risk of damage to the battery is prevented. This is achieved by monitoring and controlling the battery's charging and discharging process.

A general block diagram of a BMS is shown in Fig. 1.2. The basic task of the power module (PM) is to charge the battery by converting electrical energy from the mains into electrical energy suitable for charging the battery. The PM can either be a separate device, such as a travel charger, or it can be integrated within the portable device, as, for example, in shavers [1]. A protection Integrated Circuit (IC) connected in series with the battery is generally needed for lithium-ion (Li-ion) batteries. The reason for this is that battery suppliers are particularly concerned about safety issues due to liability risks. The battery voltage, current and temperature have to be monitored and the protection IC ensures that the battery is never operated under unsafe conditions. The battery manufacturer determines the operating conditions under which it is assumed to be safe to use Li-ion batteries. Outside the safe region, destructive processes may take place [1].

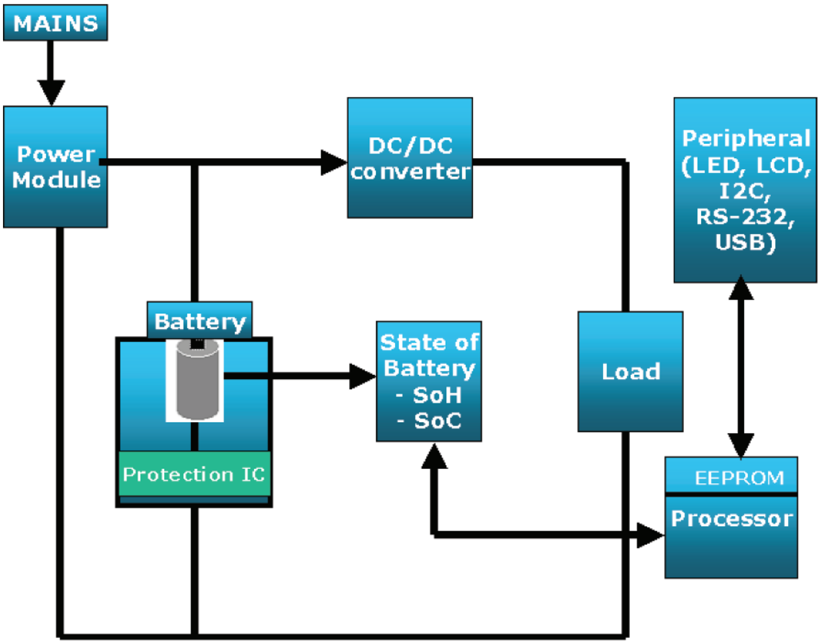

Fig. 1.2. General architecture of a Battery Management System.

The DC/DC converter is used to efficiently condition the unregulated battery voltage (3–4.2 V in Li-ion chemistry) for compatibility with stringent load requirements (see Fig. 1.2). The basic task of the load is to convert the electrical energy supplied by a battery into an energy form that will fulfil the load's function, such as mechanical energy, light, sound, heat, EM radiation, *etc*. The battery status can be indicated in one light-emitting diode (LED) or several such diodes connected in series or on a liquid-crystal display (LCD) that indicates the SoC and the battery's condition (*e.g.* the State-of-Health (SoH)) [1]. The processor is used to run the battery-management software, including the SoC algorithm (see Fig. 1.2). Communication between the BMS and other devices is another important task of the BMS. Depending on the application, various systems can be used for data exchange, such as an inter-integrated-circuit bus interface (I^2C) or some other form of serial interface (see Fig. 1.2). The battery state is used as an input parameter for the portable device's electrical management and it is an important parameter for the user. The battery state can be used to estimate the battery's expected lifetime. It can be simply described by two parameters: SoC and SoH. Both parameters depend on each other and influence the battery performance. More information on these two parameters will be given in the next section.

1.2 State-of-Charge definition

Three terms are relevant with respect to accurately implementing the monitor function of the battery state in a Battery Management System. These three terms are the State-of-Charge (SoC), the State-of-Health (SoH) and the remaining run-time (t_r). The SoC can be defined as follows:

State-of-Charge (SoC) is the percentage of the maximum possible charge that is present inside a rechargeable battery.

The SoC indication involves battery measurements and modelling [1]. As a simple example the battery voltage (V) can be measured and the *V-SoC* relationship can be stored in a look-up table function in a microcontroller [3]–[6]. The size and accuracy of the look-up tables in SoC indication systems depend on the number of stored values, *i.e.* the number of stored *V-SoC* data points. A problem is that the battery voltage changes with temperature, discharge rates and aging. Making the look-up table temperature and discharge-rate dependent can solve the first two dependencies [7]. However, aging of the battery is a complex process that involves many battery parameters (*e.g.* impedance, capacity). The process is too complex to be tackled with simple look-up table implementation [7].

The State-of-Health (SoH) is an indication of the point that has been reached in the battery's life cycle and is a measure of its condition relative to a fresh battery. The SoH can be defined as follows:

State-of-Health (SoH) is a 'measure' that reflects the general condition of a battery and its ability to deliver the specified performance in comparison with a fresh battery.

The SoH indication may involve for example cycle-counting. In the simplest case the number of full charge/discharge cycles (C_n) can be counted and the SoH can be calculated on the basis of a stored *maximum capacity*-C_n function [1]. However, a user doesn't always wait until a battery reaches an empty or a full SoC state. The system should therefore also take into consideration SoC levels other than “empty” and “full”, *e.g.* levels defined by the last discharge/charge SoC value before a user starts charging/discharging. Another problem is the spread in both battery and user behaviour. Due to this spread the SoH evolution will be different for each user and application, and will consequently be rather unpredictable. It is not possible to deal with such unpredictable behaviour with a simple charge/discharge cycles counting implementation. An adaptive system must therefore be used to ensure an accurate SoC indication when the battery ages. Examples of possible adaptive systems are neural networks [8], [9], Kalman filters [10]–[13] and fuzzy logic [14].

The SoC is usually displayed to the user in a graphic bar or in [%]. In the latter case 100% implies a full battery state and 0% the empty state. However, for a user it is convenient to know how long a portable device battery will still be able to deliver power. An SoC indication with a couple of bars does not provide sufficient information. The remaining time-of-use indication will be the most interesting and attractive solution for a portable device user. The remaining run-time can be defined as follows [1]:

The remaining run-time (t_r) is the estimated time that the battery can supply current to a portable device under valid discharge conditions before it will stop functioning.

The remaining run-time can be inferred from the remaining capacity in two ways, depending on the type of load: in the case of a current-type load the remaining capacity in mAh, so expressed as charge, is divided by the drawn current in mA and in the case of a power-type load the remaining capacity in mWh, so expressed as energy, is divided by the drawn power in mW [1]. In this book only current-type loads will be considered for simplicity.

To conclude, an accurate SoC and run-time determination method combined with a SoH calculation will improve a battery’s performance and reliability, and will ultimately lengthen its lifetime.

1.3 Goal and motivation of the research described in this book

Accurate SoC and remaining run-time indication for portable devices is important for user convenience and for prolonging the lifetime of batteries. In a survey conducted by market research group TNS involving almost 7,000 mobile users in 15 countries, over 75% of respondents said better battery life is the main feature they want from a future converged device [15]. This motivates the request for an accurate and reliable SoC, run-time and SoH indicator system in portable applications. At the moment Li-ion is the most commonly used battery chemistry in portable applications. Therefore, the focus in this book is on SoC indication for Li-ion batteries. The chosen battery in this work is Sony’s US18500G3 Li-ion battery.

Accurate SoC information allows a battery to be used within its design limits, so the battery pack does not need to be over-engineered. This allows the use of a smaller, lighter battery, which costs less. However, many examples of poor accuracy and reliability are found in practice. This can be pretty annoying, especially when a portable device suddenly stops functioning whereas sufficient battery capacity is indicated. Poor reliability of the SoC indication system may induce the use of only part of the available battery capacity. For example, a user may be inclined to recharge a battery every day, even when enough battery capacity is indicated on the portable device. This will lead to more frequent recharging than strictly necessary, which in turn leads to earlier wear-out of the battery. The effect of inaccuracy of SoC indication may be even worse when the SoC value is also used to control charging. The battery is either not fully charged or it is overcharged. In the former case, the battery will be recharged more often than needed, which will lead to earlier wear-out. In the latter case, frequent overcharging will lead to a lower cycle life [1].

Many leading semiconductor companies (*e.g.* Philips, Texas Instruments, Microchip, Maxim, *etc.*) are paying more and more attention to accurate State-of-Charge (SoC) indication. Following the technological revolution and the appearance of more power-consuming devices on the automotive electronics and portable devices markets (*e.g.* Third-Generation cellular phones) the simple SoC indication systems of the thirties based on voltage and temperature measurements [16]–[19] have been replaced by more complicated and accurate SoC systems [1], [20]–[27].

Of these, the system presented by Bergveld *et al.* in 2000 [1], [25]–[27], implementing the mathematical models described in [1], has been found to be the most accurate [28], [29]. The developed method refers to SoC estimation for a Li-ion battery. The method is based on current measurement and integration during the charge and discharge state (referred to as Coulomb counting [1], [7], [30]) and Electro-Motive Force (EMF) measurements during the equilibrium state (state in which no current is flowing into or out of the battery and the battery is fully stabilized) [1]. The EMF method is also used for calibrating the SoC system, because the same SoC level in percentage has been found for a certain measured EMF irrespective of the age and temperature of the battery. This calibration is important, because in charge and discharge states the calculated SoC will eventually drift away from the real value due to *e.g.* measurement inaccuracy in the current and the integration over time of this inaccuracy [1]. Apart from simple Coulomb counting, the effect of the overpotential is also considered in the discharge state. Due to this overpotential, the battery voltage during discharge is lower than the EMF. The value of the overpotential depends on the discharge current, SoC, age and temperature.

A couple of shortcomings of the developed method have been revealed [1]. In the first place, the implementation of an accurate battery model is essential for accurate SoC indication. The model applied in the proposed SoC indication system describes the battery EMF and overpotential behaviour, neither of which can be measured directly. Drawbacks of the measurement methods described in [1] have been discussed in [34], [35] along with possible solutions. Secondly, false entries in the equilibrium state have been detected [1]. They influence the EMF estimation and the system's calibration accuracy [1]. Furthermore, the overpotential model presents parameters that are temperature and age dependent. A better model that includes temperature and age dependence needs to be developed.

A designer of a BMS in a portable device will also be interested in the implementation requirements of the mathematical functions used in the SoC indication algorithm in a practical application. Close quantitative agreement between the results of laboratory simulations using the battery models and measurements on a real-time system in which the SoC system is implemented is then of course important. Part of the research described in this book is devoted to optimising such quantitative agreement. The optimised SoC system implementation must agree with the portable device hardware speed and memory requirements. Part of the research described in this book is aimed at finding an optimum implementation method of the SoC algorithm in a real-time system.

The final aim of the method presented in this book is to design and test an SoC indication system capable of predicting the remaining capacity of any Li-based battery and the remaining run-time with an accuracy of 1 minute or better under all realistic user conditions, including aging, a wide variety of load currents and a wide temperature range. The designed SoC indication system must moreover agree with the portable application hardware and software requirements.

1.4 Scope of this book

This book presents the results of research into battery measurements and electrochemical modelling obtained by combining the expertise of electrical engineering with that of electrochemical and computer science. The result is an adaptive method for indicating the SoC and remaining run-time that can be applied to all Lithium systems [31]–[35].

This book is organized as follows. Chapter 2 presents an overview of battery technologies and the state-of-the-art State-of-Charge (SoC) methods. The general operational mechanism of batteries and information on existing SoC indication methods will be discussed. This general information is required as a background in the remaining chapters of this book.

There are several practical methods available for SoC indication. Special attention will be paid to the SoC indication system presented by Bergveld *et al.* in [1], [25], [26], which represents the starting point of this book. This SoC system has been chosen because it is one of the most advanced SoC systems so far proposed in the literature [28], [29]. The main advantages and drawbacks of this system will be presented in Chapter 3. In chapters 4–7 improvements on this algorithm will be presented.

A complete study of a better EMF determination method developed in-house will be presented. This method will lead to a better understanding of the EMF dependence on temperature and aging and of new topics such as the EMF hysteresis. A new EMF model that includes temperature dependence will be developed. This will enable the use of the EMF at different temperatures, which will finally improve the SoC indication accuracy. A new model that predicts the EMF from the first minutes of relaxation will also be presented. Accurate EMF prediction is important because the EMF will also be used as a calibration method in our system. These efforts will be described in chapter 4.

The main drawback of the EMF method is that it does not provide continuous indication of the SoC. Therefore the SoC algorithm also uses Coulomb counting and overpotential prediction. A complete study of a new overpotential determination method also developed in-house will be presented. This method will lead to a better understanding of new topics such as overpotential symmetry and overpotential dependence on C-rate current and aging. A new overpotential model that includes C-rate current dependence will be developed. This will enable the use of the overpotential at different currents and will finally improve the SoC indication accuracy. These efforts will be presented in chapter 5.